ISSN 0010-9525, Cosmic Research, 2007, Vol. 45, No. 1, pp. 27–38. © Pleiades Publishing, Ltd., 2007.
Original Russian Text © L.L. Lazutin, T.V. Kozelova, N.P. Meredith, M. Danielides, B.V. Kozelov, J. Jussila, A. Korth, 2007, published in Kosmicheskie Issledovaniya, 2007, Vol. 45, No. 1, pp. 31–43.

# Studies of the Substorm on March 12, 1991: 1. Structure of Substorm Activity and Auroral Ions

**L. L. Lazutin[a], T. V. Kozelova[b], N. P. Meredith[c], M. Danielides[d], B. V. Kozelov[b], J. Jussila[d], and A. Korth[e]**

[a] *Skobeltsyn Institute of Nuclear Physics, Moscow State University, Vorob'evy gory, Moscow, 119899 Russia*
[b] *Polar Geophysical Institute, Kola Scientific Center, Russian Academy of Sciences, ul. Fersmana 14, Apatity, Murmansk oblast, 184200 Russia*
[c] *Mullard Space Science Laboratory, University College London, British Antarctic Survey, Cambridge, Great Britain*
[d] *Oulu University, Finland*
[e] *Max Planck Institute, Lindau, Germany*

Received April 13, 2005

**Abstract** The substorm on March 12, 1991 is studied using the data of ground-based network of magnetometers, all-sky cameras and TV recordings of aurora, and measurements of particle fluxes and magnetic field onboard a satellite in the equatorial plane. The structure of substorm activity and the dynamics of auroral ions of the central plasma sheet (CPS) and energetic quasi-trapped ions related to the substorm are considered in the first part. It is shown that several sharp changes in the fluxes and pitch-angle distribution of the ions which form the substorm ion injection precede a dipolarization of the magnetic field and increases of energetic electrons, and coincide with the activation of aurora registered 20° eastward from the satellite. A conclusion is drawn about different mechanisms of the substorm acceleration (injection) of electrons and ions.

PACS numbers: 94.30.Aa

**DOI:** 10.1134/S0010952507010042

## 1. INTRODUCTION

In this paper the substorm on March 12, 1991 is studied on the basis of the ground-based magnetic and television data, and measurements onboard the *CRRES* satellite. The high time resolution of the onboard particle spectrometers and TV recordings of aurora makes it possible to perform the study with such an accuracy which is required by the expansion processes of the substorm onset and the following activations, when several seconds are enough for the aurora picture or the flux of auroral particles to change dramatically. During a year of operation of the *CRRES* satellite where the successful selection of detectors was combined with the orbit leaving the satellite near the equator in the quasi-trapping region for a long time, aurora was registered near the region conjugated to the satellite location only twice. In the first case [1], the satellite was located eastward from the emission flashes, which made it possible to study the geometry of the region of electron acceleration. In our case, the satellite was at first to the west of the activity epicenter, and then the auroral surge of WTS (westward traveling surge) reached and covered the satellite. The spectrum of processes available for studying was in this case much wider. The detailed space–time structure of the disturbance and the relation of the processes of growth phase and beginning of the expansion to the fluxes of auroral ions are studied in the first part of the paper. The second part [2] is dedicated to the problems of acceleration (injection) of auroral electrons.

The ion dynamics in the quasi-trapping region where a substorm begins plays a leading role in the preparation and development of the substorm: just the drifting ions provide the main contribution to the partial ring current changing the magnetospheric configuration, while the plasma pressure gradients determine the structure of field-aligned currents [3, 4]. At the same time, the dynamics of auroral ions is poorly known. The information is mainly obtained from averaged statistical data. There are few publications considering the ion dynamics with a good time resolution, and no studies were made with acceptable spatial resolution. Since both the satellite and the region covered by the disturbance were in the inner magnetosphere, in the quasi-trapping region, we say nothing about the processes in the magnetosphere tail which could have taken place there.

## 2. OBSERVATIONS

The ground-based observations included a network of magnetic stations in Scandinavia and Russian North, three all-sky cameras with a resolution of 1 min, and the television camera of aurora in Kilpisjarvi with a standard resolution of 24 frames per second. The station coordinates are presented in Table 1, some of them are also shown in Fig. 1. The calculated projection along

**Table 1.** Coordinates of the ground-based observatories, deg

| Abbreviation | Station | Geographic latitude | Geographic longitude | CGM latitude | CGM longitude |
|---|---|---|---|---|---|
| APA | Apatity | 67.58 N | 33.31 E | 63.86 N | 112.9 E |
| BJN | Dear Island | 74.50 | 19.20 | 71.45 | 108.07 |
| BOR | Borok, CIS | 58.03 | 38.33 | 54.06 | 113.41 |
| DIK | Dixon | 73.5 | 80.6 | 68.3 | 155.9 |
| FAR | Earoes | 62.05 | 7.02 W | 60.72 | 77.44 |
| KEV | Kevo | 69.76 | 27.01 | 66.32 | 109.24 |
| KIL | Kiplisjarvi | 69.02 | 20.79 | 65.88 | 103.79 |
| LOZ | Lovozero | 67.97 | 35.08 | 64.23 | 114.49 |
| MUO | Muonio | 68.02 | 23.53 | 64.72 | 105.22 |
| NOR | Nordli, Norway | 64.37 | 13.36 E | 61.50 | 94.92 |
| NUR | Nurmij rvi | 60.50 | 24.65 | 56.89 | 102.18 |
| OUJ | Ouluj rvi | 64.52 | 27.23 | 60.99 | 106.14 |
| PEL | Pello | 66.90 | 24.08 | 63.55 | 104.92 |
| SOD | Sodankyl | 67.37 | 26.63 | 63.92 | 107.26 |
| TRO | Tromso | 69.66 | 18.94 | 66.64 | 102.90 |
| YMN | YanMayen | 70.90 | 8.70 W | 70.29 | 82.93 |

the field lines of the *CRRES* satellite location (dashed curve) is also shown there. The *CRRES* satellite was launched on July 25, 1990 to a transition geosynchronous orbit with a period of 14 h, perigee of 305 km, apogee of 35768 km, and inclination of 18°. Several detectors of particles operated onboard the satellite, out of them we use the LEPA (low energy plasma analyzer) block which measured electrons and ions in 20 differential energy channels within the range 100 eV < $E$ < 30 keV and the pitch-angle distribution with a resolution of 5.625° × 8° from 0° to 180° every 30 s of the satellite rotation around its axis [5].

The detector of energetic particles EPAS (electron–proton angular spectrometer) measured electrons in 14 channels within the range 21–285 keV and ions with energies of 37 keV–3.2 MeV in 12 channels [6]. The energy thresholds of the channels are presented in Table 2. The data of the fluxgate magnetometer [7] were available with averaging over 2 s. The measurements of the electric field were also available but were not suitable for a detailed analysis, since the time resolution was determined by the slow rotation of the satellite and was equal to 30 s.

### *2.1. Analysis of Substorm Activity*

One can see in the graphs of the $A_e$ index presented in Fig. 2 that the day of March 12, 1991 was moderately disturbed with a few substorms of increasing intensity. The times of the commencement of the substorm we are interested in at 20:26 UT and of the expansion at 20:30 UT are shown with the double dashed line (universal time is used here and in what follows).

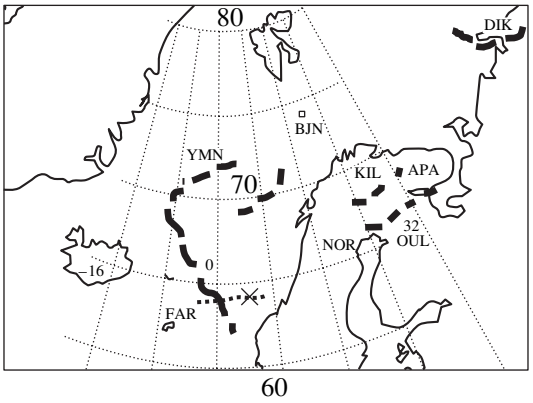


**Fig. 1.**

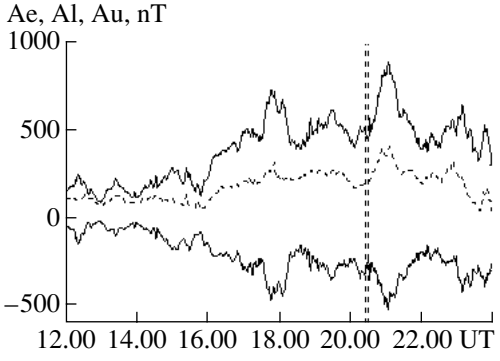


**Fig. 2.**

The substorm developed on a disturbed background and was rather strong but with a gradual development: the $A_e$ index increased during half an hour up to 21:00 UT and reached a value of 500 nT. One can see in Fig. 3 where the $H$ components of several magnetometers are presented that this gradual development includes a series of activations scattered over the Scandinavian midnight sector.

The present-day substorm theory considers as important the $T_0$ moment of the expansion phase onset. For identification of $T_0$ we could use all basic methods: using the beginning of the train of Pi2 pulsations, the breakup of the aurora equatorial arc, the sharp beginning of the negative magnetic bay, and the beginning of dipolarization of the magnetic field and injection of energetic electrons into the geostationary region. We have to confess that we obtained no unambiguous result.

The train of Pi2 pulsations detected at the Borok observatory and presented in Fig. 4 begins at 20:22 UT with an increase in the amplitude until 20:30 UT, which confirms a gradual and multi-step character of the substorm development. The analysis of magnetograms and aurora recordings shows, however, that at 20:22 UT (moment $A$) only the activation of the auroral arc was observed, and due to this feature it can be referred to as a disturbance of the pseudo-breakup type.

The detailed analysis of the TV recording which, unfortunately, can not be reproduced here shows that

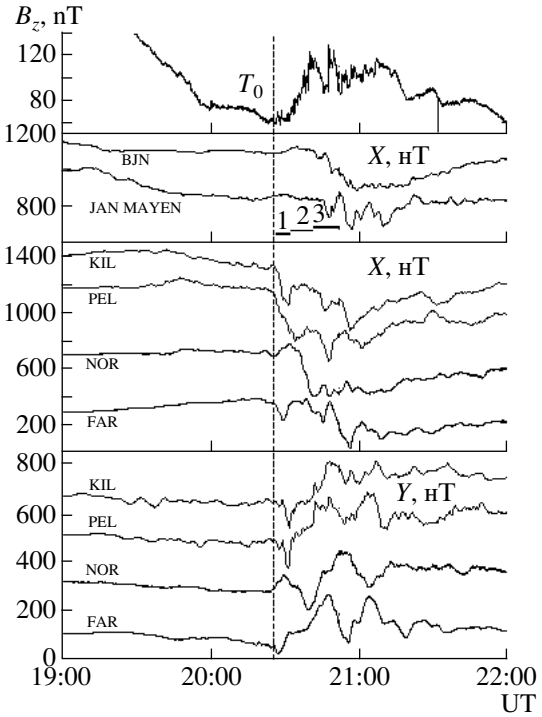


**Fig. 3.**

**Table 2.** Energy channels of the EPAS electron (E) and ion (P) detectors, keV

| | | | |
|---|---|---|---|
| E1 | 21.5–31.5 | P1 | 37–54 |
| E2 | 31.5–40 | P2 | 54–69 |
| E3 | 40–49.5 | P3 | 69–85 |
| E4 | 49.5–59 | P4 | 85–113 |
| E5 | 59–69 | P5 | 113–147 |
| E6 | 69–81 | P6 | 147–193 |
| E7 | 91–94.5 | P7 | 193–254 |
| E8 | 94.5–112 | P8 | 254–335 |
| E9 | 112–129.5 | P9 | 335–447 |
| E10 | 129.5–151 | P10 | 447–602 |
| E11 | 151–177.5 | P11 | 602–805 |
| E12 | 177.5–208 | P12 | 805–3200 |
| E13 | 208–242.5 | | |
| E14 | 242.5–285 | | |

the activation was of the rotational type: an eddy increase in brightness manifesting generation of a jet of the field-aligned current flowing out from the ionosphere is formed on the arc. The earlier increases in the arc brightness (seen in the keogram in Fig. 5) had similar features.

At the same time, at 20:22–20:24 UT a small decrease in the $X$ component is detected by the PEL, KIL, and APA magnetometers manifesting an increase in the westward electrojet that remained small till the sharp increase at the active phase commencement.

Some increase in the luminosity background in the region of the southern arc is observed at 20:24 UT, while according to the measurements at three Finnish all-sky camera, the breakup of the equatorial arc began at 20:26 UT. At the same moment the magnetogram at the Apatity station detects a sharp beginning of the negative bay, so there are all grounds to believe that the substorm begins at $T_0$ = 20:26 UT.

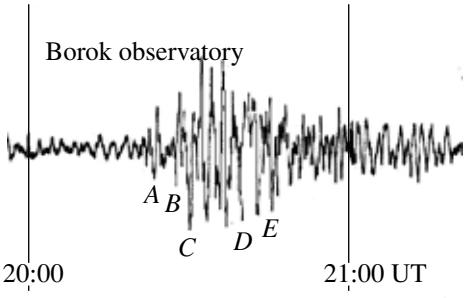


**Fig. 4.** (*A*) is the pseudo-breakup; (*B*) is $T_0$, (*C*) is $T_1$, (*D*) is the breakup at Dikson, and (*E*) is the local activation at the *CRRES* meridian.

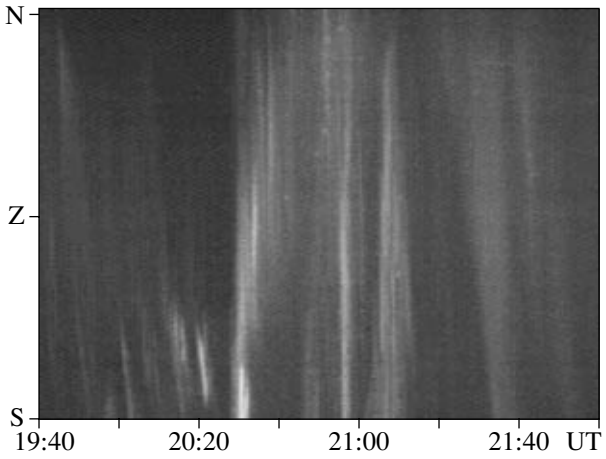


**Fig. 5.**

The TV camera at Kilpisjarvi detects the luminosity at about 15° over the horizon, so the breakup at the $T_0$ moment is not seen in the keogram. The keogram based on these data is presented in Fig. 5.

A breakup in the aurora is seen at $T_1$ = 20:28 UT in the keogram, and it is even better seen in the TV record. The aurora bursts appearing in the arcs moving equatorward before this second breakup can be reasonably ascribed to the growth phase of the substorm. And, finally, the third significant time mark $T_D$ = 20:30 UT is associated with the commencement of the quick poleward activity expansion and beginning of the large-scale dipolarization of the magnetic field, these events also being often related to $T_0$ (see the increase in *CRRES* $B_z$ in Fig. 3).

Several images of the aurora corresponding to three moments $T_0$, $T_1$, and $T_D$ are presented in Fig. 6. Not going into a detailed description of the activity development, one can say that it developed exponentially: at first small activation at the end of the growth phase and the breakup $T_0$ in the southern arc with a limited expansion, and then with accelerated large-scale expansion after the second activation. Such a division of the substorm commencement into slow and quick phases is not new and was described in [8–10]. It was assumed that the slow phase is caused by a balloon instability, while the rapid phase is determined by a series of current discontinuities and local current reconnections onto the ionosphere [11].

A westward motion of the activity is observed after 20:34 UT and, though the aurora was not already observed there, no differences from typical schemes are seen in the magnetic data: the western edge of the surge formed a N–S front of the WTS which in two jumps moved westward in the 20:41–20:47 UT interval. The second such jump coincided with the local activation detected onboard the *CRRES* satellite. The analysis of the current system structure (not presented here for the

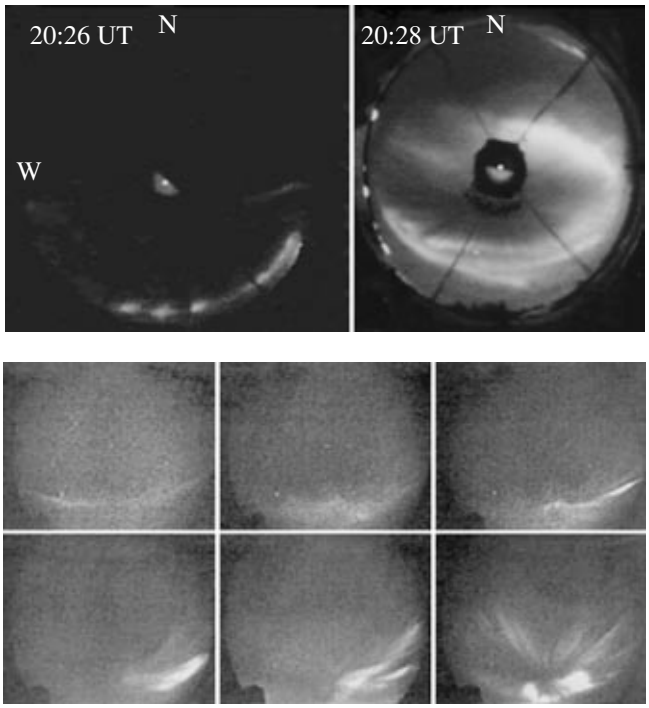


**Fig. 6.** Photos of the aurora: at Muonio station at the moment $T_0$ (the left-hand side) and at Oulu station at the moment $T_1$ (the right-hand side). The development of the breakup $T_1$ and $T_D$ according to the photos at Kilpisjarvi is shown at the bottom.

sake of brevity) shows that the WTS front at this time coincided with the magnetic meridian of the satellite.

The eastward development of the activity is different from the westward one, and in our case no consequent expansion eastward is seen at all. A sharp beginning of a negative *H* bay is detected by the Dixon station at 20:40 UT (Fig. 3), while at the meridians of Apatity and Sodankyla, the poleward expansion almost ended already, but the westward motion continued.

The *LANL-095* geosynchroneous satellite located at the meridian of Dixon at 20:10 UT detects the beginning of the decrease in energetic particles (electrons and ions) and then from 20:16 to 20:40 UT a strong decline (dropout) showing that the magnetic field lines are stretched there into the tail and the quasi-trapping boundary has been displaced to the Earth. All this is a typical feature of the growth phase (Fig. 7). The vertical dashed lines in Fig. 7 show the moments of the substorm commencements and local activation in the Scandinavian sector. One can see that there is no reaction in the *LANL* particle fluxes. Thus, during the development of the main western substorm, the growth phase continues in the early dawn sector leading to a commencement of a new independent substorm. As a result, for some time we observe simultaneously the active phase of two substorms in different longitudinal sectors.

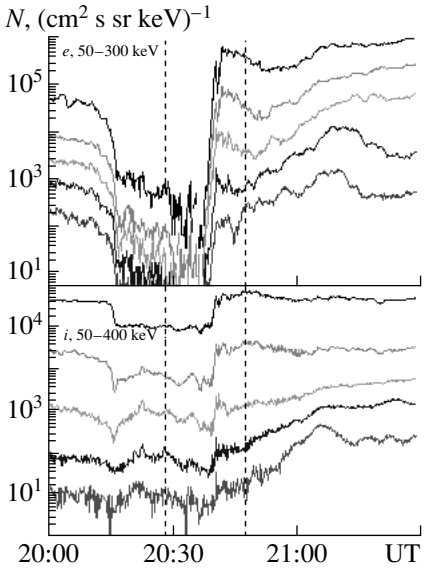


**Fig. 7.**

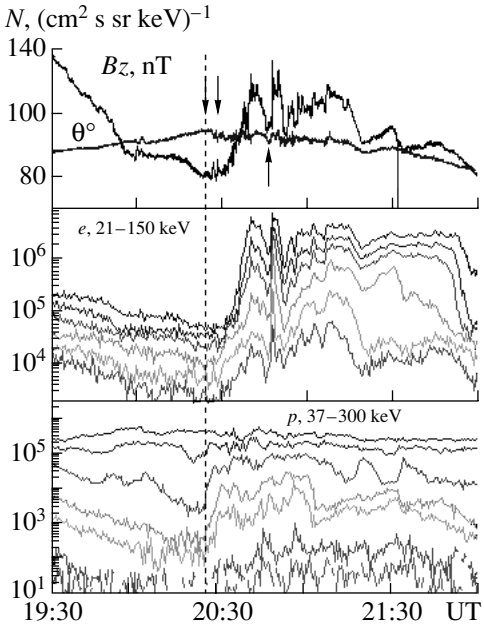


**Fig. 8.**

### *2.2. The CRRES Satellite, Auroral Ions*

Within the interval 20:00–21:00 UT on March 12, 1991, *CRRES* was located in the vicinity of the equatorial plane at 6.0–6.6 $R_E$ with the calculated projection of the magnetic field line located between Scandinavia and Great Britain (Fig. 1). The satellite moved from the Earth and reached the inner boundary of the plasma sheet at about 19:45 UT. There, in the central plasma sheet in the region of quasi-trapping, the main events considered in this paper occurred.

The summary graphs of the measurements of the magnetic field and energetic particles onboard the satellite are presented in Fig. 8. Two arrows at the left-hand side show the moments $T_0$ and $T_1$. We remind that at the breakup moment the satellite was located 20° to the west from the point of the substorm commencement. It would be, certainly, more interesting if this distance was absent. However, one should not dramatize the situation. An instant response to the breakup beginning in the form of a disturbance in the *H* component of the magnetic filed is seen at many stations including the stations located near the satellite meridian. In the magnetogram of the satellite, we also see two bursts of the magnetic field at about $T_0$ and $T_1$. One can also see in the photo of the aurora that the arc is activated in a wide belt of longitudes. Therefore, a joint analysis of the substorm activity and particle dynamics onboard *CRRES* makes sense, especially for the ions drifting westward.

When the activity in the form of WTS covers the satellite meridian (the third arrow in the graph), an analysis of the fine structure of the dynamics of auroral electrons presented in the second panel of this figure becomes possible.

Figure 8 demonstrates a typical pattern of the dynamics of energetic particles for the satellite in the region of the substorm activation in the quasi-trapping region. A decrease in the intensity is observed in all energy channels till 20:20 UT. It is caused by the satellite motion to the boundary of the outer radiation belt and by simultaneous variation in the magnetic field configuration due to the extension of the field lines into the tail at the growth phase of the substorm. The considerable increase in the electron flux that began at the moment of dipolarization $T_D$ is a well-known typical pattern of the substorm injection. Considerable difference in the time of injection of ions and electrons is not a new effect [12–14], however, poorly known. The ion flux begin increasing (dashed line) before the substorm commencement at $T_0$ and reaches a maximum before the dipolarization beginning. We consider this effect in more detail below.

*Fine structure of the ion injection.* Figure 9 presents the time behavior of the ion fluxes in a few energy channels from 20:20 to 20:34 UT (at the last minutes of the growth phase and the first minutes of the active phase of the substorm). The detectors scan in sequence the particle fluxes with various pitch-angles, and the sinusoid seen in some parts manifests the pitch-angle anisotropy of the particle flux. First of all, a considerable discrepancy in the variations of the particle fluxes in different (often adjacent) energy channels is seen, the variations occurring sharply, in jumps. The moments of such variations are marked with vertical dashed lines. At 20:22 UT the pitch-angle distribution (PAD) in channels P5–P6 changes, while an increase in the fluxes at all pitch-angles is seen in P2 channel. An increase in the intensity in P3–P5 channels begins at 20:24 UT, at

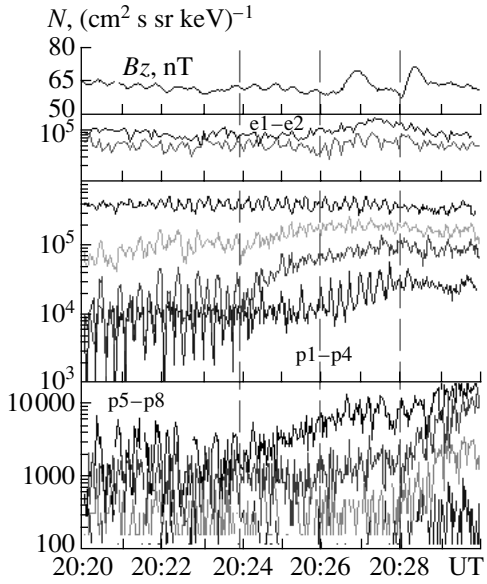


**Fig. 9.**

20:26 UT PAD changes in channel P4 and the intensity in channels P6–P7 increases, and, finally, at 20:28 UT a new increase in the intensity is observed in higher channels P6–P11. It is worth noting that all the times indicated have been already mentioned earlier when (analyzing the substorm development in the aurora and magnetic field) we noted the intervals of activations and also the moments of active phase beginning $T_0$ and $T_1$. There is no clear certainty in these coincidences, both the forms of aurora activation and variations in the particle distribution function are numerous, nevertheless, it is the only feature allowing one to search for causes of variation in the ion fluxes.

*PAD of energetic ions.* Figure 10 illustrates the transformation of the pitch-angle distribution of ions. Each distribution is a result of averaging over 20–30 s beginning from the time moment indicated in Fig. 10. In the first section, we have seen that only low-energy ions have a trapped distribution before 20:23 UT, while the butterfly-type distribution with a dip in the vicinity of 90° is observed in higher channels. This picture is typical for trapped protons at the periphery of the trapping region, the extension of the field lines into the tail at the growth phase intensifies such a structure of PAD.

Then the dip at 90° is filled in less than a minute and the majority of the channels show a pancake distribution. It is worth noting that *CRRES* detects no variations in the magnetic filed in this interval, so there is no simple answer to the question on the source of such variation or acceleration mechanism. The pancake distribution is conserved till $T_0$. The degree of the anisotropy decreases, and in 1–2 min after $T_0$ almost isotropic distribution is recorded.

*Energy spectrum of ions.* The spectrum of energetic ions (90° and 145°) for three time intervals is shown in Fig. 11. A depression in the captured particles flux is observed till 20:20 UT due to the specific butterfly-type distribution over pitch-angles discussed above. After the acceleration between 20:23:45 and 20:25:00 UT, the fluxes of trapped ions in P3 and P4 channels have increased by a factor of 10, and the spectra of ions with pitch-angles of 90° and 145° become similar. The third interval is related to 20:28 UT when the monotony of the spectrum was distorted by the increase in ions with an energy of 100–300 keV, both trapped and field-aligned. Joint spectral curves in the energy interval 0.1–500 keV according to the data of two detectors of the satellite are presented in Fig. 12. Only the data on trapped particles were taken, since for low-energy ions (< 30 keV) the flux of field-aligned particles is considerably lower during the entire period of substorm activity.

The spectrum has a wide maximum or inflection point in the region of 15–50 keV, and the ion flux does not vary strongly in this region. In the region of low energies, the variability is high. Further consideration of the ion dynamics will be made upon passing from particle fluxes to energy density or pressure.

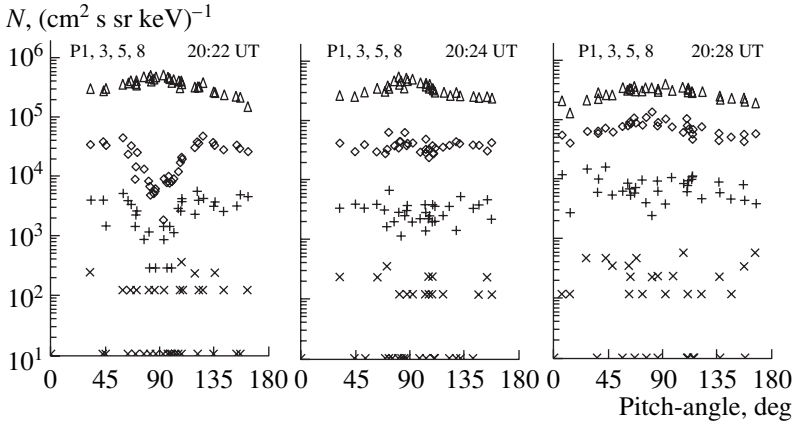


**Fig. 10.**

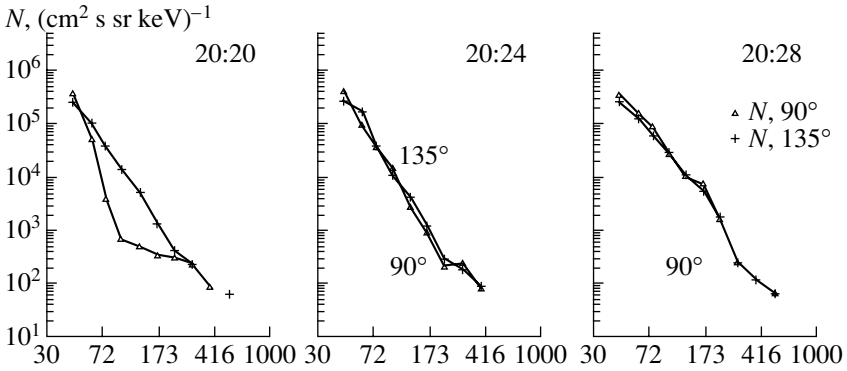


**Fig. 11.**

*Plasma pressure and the magnetic field.* The main parameter determining the structure and dynamics of a plasma configuration is the plasma parameter $\beta = 2\mu_0 p/B^2$, where $p$, $B$, and $\mu_0$ are the plasma pressure, magnetic field strength, and permeability of the vacuum, respectively.

We have calculated the total plasma pressure in the range 0.1–600 keV and the partial pressure for particular parts of the energy spectrum of ions. The comparison of the plasma pressure to the density of the magnetic field energy is presented in the upper panel of Fig. 13. The lower panel of Fig. 13 shows the behavior of the partial pressure of ions with energies of 0.1–15 keV, 37–54 keV, and 70–600 keV. It is worth noting that the absolute values can be inaccurate, because we neglected the contribution of electron fluxes and field-aligned ions to the pressure and did not take into account the diamagnetic effect.

Till 19:45 UT the plasma pressure is lower than the magnetic field pressure and is determined mainly by trapped energetic ions. After that the satellite enters the plasma sheet heated by the previous activity, and the plasma pressure begins to grow due to particles with the energy lower than 30 keV and becomes higher than the magnetic pressure. At the growth phase, the plasma parameter has a value of 2–3 even without taking into

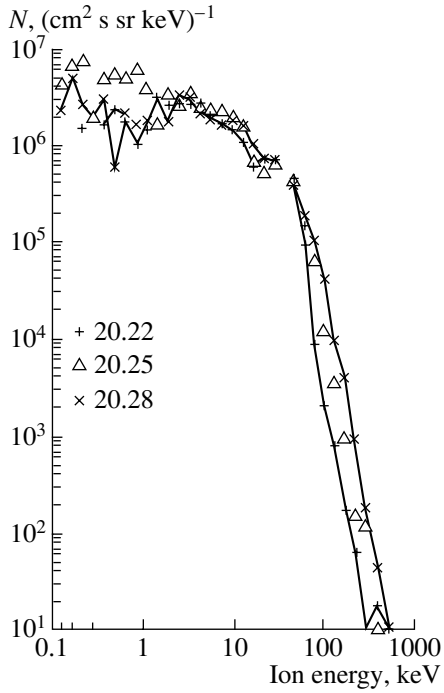


**Fig. 12.**

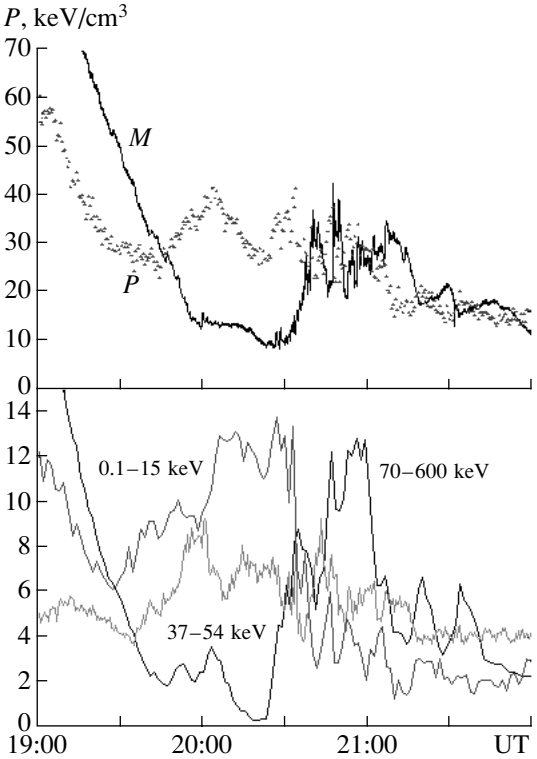


**Fig. 13.**

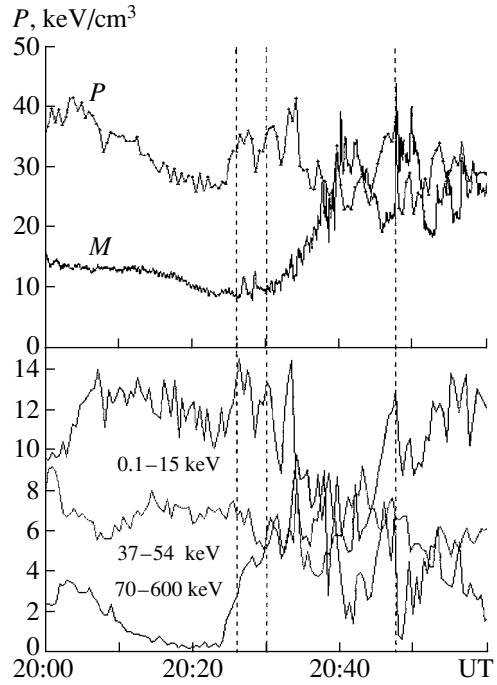


**Fig. 14.**

account the contribution of field-aligned particles. The maximal value $\beta = 4$ is observed before the beginning of the large-scale dipolarization. Then the ratio of pressures decreases and undergoes deep variations to both sides from the $\beta = 1$ value.

Let us consider these variations using Fig. 14 where the same graphs of the pressure are shown in the scale extended in time. The dashed curves corresponding to the moments $T_0$ and $T_D$ and to the local activation at the satellite meridian at 20:47 UT coincide with the maximal values of the plasma pressure. Thus, the activation consists of two parts: at first the pressure growth (the ion flux growth) and then its sharp decrease at the moment of the beginning of the magnetic field dipolarization. Such a structure is seen around $T_0$ and $T_1$, in the activations at the moment of the expansion beginning $T_D$, and especially clearly it is seen at 20:47 UT, when *CRRES* is located near the activation center. The short-period pressure increase with a maximum at 20:34 UT coincided with no ground-based manifestation of the substorm mentioned earlier. However, turning to the TV records of the aurora we made sure that there also the aurora became brighter.

Now we come to the bottom parts of Figs. 13 and 14 and consider the relative contribution of the CPS plasma ($E < 15$ keV) and energetic ions ($E > 70$ keV). One can see that the total contribution of the energetic ions to plasma pressure decreases till 20:24 UT, that is, till the beginning of the pre-breakup activations discussed above, and then increases during the entire duration of the active phase. On the contrary, the contribution of CPS plasma decreases considerably with the beginning of the active phase. At the same time, the above-noted pressure increases prior to the activations and the following decrease are caused by both low-energy and high-energy components of the ion population. We note also that ions of moderate energies conserve approximately constant intensity level, and their variations occur in anti-phase with the variation of energetic particles.

## 3. DISCUSSION OF RESULTS

### *3.1. Substorm*

The commonly used model of a substorm consists of several successive elements: the magnetosphere accumulates energy changing its configuration (the growth phase), an explosive beginning of the expansion or active phase is observed at the moment $T_0$, and then the magnetosphere returns to its previous state (the recovery phase). In spite of the fact that this scheme was repeatedly criticized, corrected, and complemented, for the majority of investigators (especially those who were not involved in a detailed analysis of experimental data) it remains the main background for drawing their own picture of the disturbed magnetosphere.

At the same time, the corrections are significant. First, the absolute importance of the unique explosive beginning $T_0$ was called into question. Substorms with multiple beginning get their rights for existence in the joint publication of the experts on substorms as long as a quarter of a century ago [15]. The fact that the activation of aurora begins still at the growth phase is known to any observer of aurora. The two-step scheme of the active phase beginning consisting of the initial slow stage without considerable expansion and the second fast stage was used in many case studies and review papers [10, 16]. Second, the active phase, the expansion of aurora, covers usually a small longitudinal sector with an average dimension of 30° and outside it the growth phase can continue. Finally, third, one should not insist on the obligatory strict time succession of substorm phases. The loading and unloading of energy may be observed simultaneously, in particular, spontaneous substorm onsets do not lead to a considerable expansion and may be once again continued by the growth phase.

The experience in the analysis of a large number of substorms shows that instead of the scheme of an elementary isolated substorm shown in the top part (a) of Fig. 15, it is more correct to use the scheme b presenting coexistence of global processes of energy loading, magnetosphere relaxation, and localized activations. The important turning point is not necessarily related to the beginning of the first activation $T_0$, but rather to the beginning of the large-scale expansion $T_D$.

For the analysis of observations with a poor time resolution (for example, the detection of the auroral oval onboard the *Polar* satellite), the scheme of succes-

sive phases of an elementary substorm is more appropriate, since individual activations disappear, are blurred, and seem as insignificant details, and only the dynamics of the large-scale structure is seen. In our case, neglecting "details" one would not be able to clarify the main problem of the ion dynamics, therefore, the interpretation of the ground-based observations on the basis of the bottom scheme is preferable.

Indeed, the activations during the substorm on March 12, 1991 begin still at the growth phase, the poleward expansion increases exponentially at first being slow and limited in latitude and then rapidly and far to the quasi-trapping boundary.

The analysis performed makes it possible to agree with the two-step scheme of the substorm commencement. At the $T_0$ moment the equatorial arc of aurora is activated splitting into separate bright segments, which is in agreement with the model of balloon instability development [17, 18]. The second activation $T_1$ is more powerful, explosive, and it can quite correspond to the instability of the current discontinuity type [11, 19].

Finally, the discovered effect of development of two substorms in different longitudinal sectors (at one growth phase, though not in a sequence of one after another, as a continuation and consequence, but with overlapping, with simultaneous development of active phases at some time interval) falls into this pattern.

### *3.2. Substorm and Ion Fluxes*

1. The major part of the substorm effects attracting attention of scientists is related to auroral electrons. The accelerated auroral electrons produce all the bright effects of the aurora, electron precipitation causes ionospheric effects, radiowave absorption, electrojet and magnetic disturbances, bursts of the VLF emission, pulsations, etc.

The role of ions in the development of substorm disturbances is less spectacular, but not less important. Electrons are frozen in the magnetic field and cannot change its configuration considerably, while ions as the main carriers of current in the auroral magnetosphere are responsible for changes in its configuration. The anisotropy of plasma pressure governs the field-aligned currents, an increase in the plasma parameter $\beta > 1$ leads to a destabilization of the magnetic trap and provides favorable conditions for a development of explosive instability of a substorm (see, e.g., [20]).

The very diversity of the expansion phases of a substorm indicates to existence of an invisible factor, the agent controlling the dynamics of the active phase. Ion fluxes are, most probably, such an agent.

2. Though protons or ions in the auroral magnetosphere (in quasi-trapping region, in the geostationary region) are often considered as one population (ions of the plasma sheet), the analysis of direct measurements presented above is in favor of splitting protons into, at least, two groups: the low-energy ions of CPS and energetic quasi-trapped ions with the boundary between them somewhere between 30 and 70 keV. Konradi et al. [21] proposed to split the substorm ions into three parts: above 40 keV, between 2 and 40 keV, and below 2 keV. Probably, the third gradation should be actually introduced, since we saw the specific character of partial pressure variations within this energy range. On the other hand, the relative constancy of the particle flux in this region may be explained by the fact that the increment of particles due to acceleration of low-energy ions is compensated there by the transition of the same number of ions into the group of energetic particles.

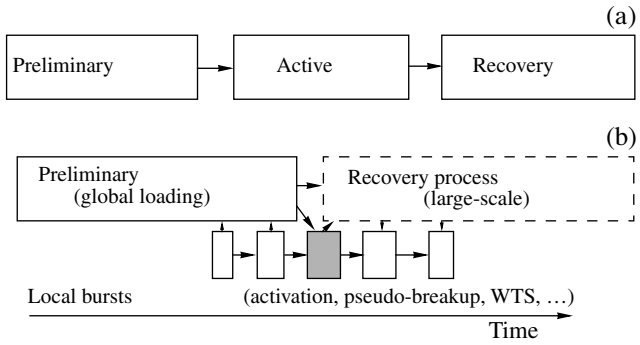


**Fig. 15.**

One can see in the pressure graphs that ions of low and moderate energies begin to be heated with the beginning of the growth phase, and the plasma pressure grows exactly due to these particles. Energetic ions become involved later, at the end of the growth phase, and their intensity increases with each new activation. The fluxes of low-energy ions, vice versa, decrease with the beginning of the active phase. At the same time, before the activation, the short-period increase in the low-energy component occurs synchronously with the energetic component (the analysis of the lower-energy part of ions ascribed here to CPS, will be in more detail presented elsewhere).

3. Direct measurements in the magnetosphere are the only reliable source of information on the fine structure of auroral ion fluxes. Low-orbiting satellites pass the auroral region too quickly and cannot follow the development of activations in time. Moreover, these satellites simply would not detect an increase in ions if only the particles trapped in the vicinity of the equator plane are accelerated, as it was the case during the considered substorm at 20:24 UT.

There are proton emissions in aurora, but they have a weak intensity and are located close to bright emissions excited by electron precipitation, so that their identification requires long (about a minute) exposure. There were some attempts to reveal a character of proton aurora variations during substorms. In particular, it was reported in [22] that proton aurora decays after the beginning of the active phase of a substorm. It was

found in [23] that an intensification in the proton $H\alpha$ emission is observed 2–4 min before the beginning of the active phase.

Both the features agree with the changes described above. The flux of ions with the energy <30–70 keV with which proton aurora may be associated actually decreases after $T_0$. As for the enhancement in proton emission before the activation beginning, it is in direct correspondence to the effect of ion pre-increase.

4. Recognizing the difference in dynamics of ions and electrons, one can easily assume that the acceleration of these groups of particles in a substorm should occur in a different way and under the action of different physical mechanisms. At the same time, for a long period and until now, the injection of electrons and protons is considered as a joint acceleration process due, for example, to dipolarization of the magnetic field.

Indeed, at the time resolution of more than a minute, a decrease of the intensity of ions and electrons at the growth phase occurs simultaneously or almost simultaneously, so that the increases in the beginning of the active phase also look as a joint process. In our Fig. 8 the increases in energetic ions and electrons overlap and only the very beginnings are shifted.

Studying the interrelation between the injection of protons and electrons, Birn et al. [24] concluded that in the midnight sector they are observed simultaneously, in the dusk sector protons on the average increase with an advance of 2 min, and in the dawn sector electrons increase earlier. Theoretically, this result does not contradict the joint acceleration concept and can be explained taking into account the opposite directions of the magnetic drift of ions and electrons.

However, at detailed studies of individual substorms with a good resolution, it was reported in [12, 13, 25–27] that the flux of energetic ions increased before the local dipolarization in the pre-midnight sector and before the increase of electrons.

A special study of more than ten substorm activations according to the *CRRES* satellite data [14] showed that the burst of ions almost in all cases actually occurs ahead of dipolarization of the magnetic field and the local increase in electrons by the time from a few to 20 seconds, and sometimes by more than a minute. It was also shown that ions increase within a limited energy interval and that the energy grows in repeated bursts. It was assumed that the ion acceleration is of a resonant character.

Thus, we come to the conclusion that the injection of energetic ions during a substorm is not a consequence of some unique acceleration process, but presents an aggregate, sequence of acceleration acts at separate substorm activations. The auroral electrons are also accelerated during activations, however, most probably, with a shift in time. The ions begin to increase before the beginning of dipolarization, while the acceleration of energetic electrons begins simultaneously with dipolarization. It follows from this time shift that there are different mechanisms of acceleration of ions and electrons, and that they operate alternately. We do not describe in detail what "activation" is, in itself it includes brightening and poleward broadening. It may be that the beginning of the increase in ions occurs at the brightening stage and continues at the broadening stage. Other versions of the interpretation are also possible. One cannot exclude a spatial shift of the regions of electron and ion acceleration, however, the main conclusion on different mechanisms of ion and electron injection remains valid. The total effect of a dozen and more activations creates an almost simultaneous picture of the injection of ions and electrons. The discrepancies in the time structure of proton and electron injections and (not always observable) initial shift were considered as insignificant details, and the presence of some joint mechanism of injection of ions and electrons raised no doubts.

5. The problem of a mechanism of the auroral ion acceleration is of primary importance for understanding the nature of substorms and magnetic storms. An asynchronous character of the variations of fluxes in different energy channels shows that one should look for mechanisms accelerating ions within a limited energy range. One should not draw definite conclusions on the basis of a few coincidences, however, it is likely that small activations in aurora and increases in ions are mutually related and that on these very activations the pumping up of the ion energy occurs. During the local activation in the vicinity of the *CRRES* orbit (it will be analyzed in the second part of the paper), the ion pressure increase before the dipolarization coincided with the bursts of field-aligned fluxes of low-energy electrons. We have already drawn attention to a rotational character of flashes of the elements of aurora arcs. This fact can indicate to generation of circular structures of the induction electric field which is able to accelerate selectively the ions with close values of the Larmor radius.

6. The plasma pressure, its spatial distribution, gradients, and dynamics are one of the main factors governing the structure and dynamics of the magnetosphere [28]. In this connection, the quick changes in the pressure, its growth, and decrease prior to and after an activation should be considered as determinative processes of a magnetospheric substorm. The energy density of energetic ions before the activation exceeds the energy density of the magnetic field, this fact being able to trigger development of an instability. A quick grow and decrease of the plasma density distort monotonous character of the Earthward plasma pressure gradient, and at the segments of gradient reversal an eastward current appears whose existence is postulated in some models of a substorm.

The decrease in the main current may be related also to the changes in the pitch-angle distribution of ions

[29]. In the stationary plasma, the total current is described by the following expression

$$j_\perp = c\left(\frac{[\mathbf{B}\nabla p_\perp]}{B^2} + \frac{(p_\parallel - p_\perp)}{B^2}[\mathbf{B}(\mathbf{b}\nabla)\mathbf{b}]\right).$$

The second term in the right-hand side is determined by the anisotropy of pressure and by the radius of curvature of the magnetic field lines. Within the interval 20:20–20:24 UT a transition from $P_\parallel > P_\perp$ to $P_\parallel = P_\perp$ is observed. This leads to a decrease in the current if the first term does not change considerably.

Thus, there is a ground to assume that there is if not a discontinuity, then a strong weakening of the westward current which is followed by (postulated in many models) appearances of the current wedge of a substorm, induction field, etc.

7. Any study of a particular substorm has its weak points, as a rule, due to insufficient set of experimental data. In our study the data bank was large, and the substorm description presented above is only an abstract of the initial analysis. Nevertheless, there are some weak points, mainly because of the absence of additional direct measurements in the magnetosphere.

Among the problems that cannot be solved on the basis of measurements at one point, the problem of spatial characteristics of ion increases is principal. If energetic ions are accelerated at local activations of aurora, then how can one explain the coincidence of the ion dynamics with the aurora in the region located westward from the satellite by 20° within the period 20:22–20:30 UT? The drift velocity is not high enough, and then one would see a dispersion in energies, which is absent. It remains to be assumed that the disturbance is transferred quickly, for seconds. Generally speaking, quick propagation of disturbances along auroral arcs is supported by visual observations.

An activation simultaneously or very quickly propagating along an arc in the form of bright fragments AAF (Auroral Arc Fragmentation) is one of base blocks of a substorm in aurora [30]. This very character of auroral arc decay at the $T_0$ moment is seen in the photo of the aurora in Fig. 7. In that way the effective distance between the meridian of the satellite and the activation region shortens considerably.

## 4. CONCLUSIONS

In the first part of the study of the substorm on March 12, 1991 and particle dynamics in the magnetosphere, the main attention was paid to the analysis of the substorm structure and the behavior of auroral ions. The main conclusions are as follows.

1. The analysis of the ground-based observations showed that the considered disturbance had the following features: its activity increased exponentially or had a two-step character. The slow part began still at the growth phase and included moments $T_0$ and $T_1$ of the increase in the brightness of the equatorial and the next-to- pole auroral arc. The quick part began at the moment $T_D$, i.e., in the beginning of the large-scale poleward expansion. In the sectors of the auroral zone distanced along longitude, two substorms united only by a common growth phase were observed.

2. The population of ions in the nighttime sector of the quasi-trapping region, in the vicinity of the inner boundary of the central plasma sheet, should be split into two parts with a different character of variations. The pressure of low-energy ions of CPS grows with the beginning of the growth phase, transfers the plasma parameter into the region $\beta > 1$, and after the beginning of the expansion phase the contribution of low-energy ions decreases. The energetic quasi-trapped ions begin to grow at the last minutes of the growth phase and continue to grow during the expansion phase increasing their contribution to the total balance of the plasma pressure. During the active phase, the plasma parameter $\beta$ is jumping: it decreases or increases depending on the current situation (a growth or fall of the activity).

3. The increases in the pressure $\beta$ in the beginning of the activation are related to the increase in the ion flux, while the decrease in $\beta$ is due to the decrease of the intensity immediately after the beginning of the dipolarization and an increase in the burst of energetic electrons. The increase and the following decrease of the intensity are observed for both the energetic and low-energy part of ions. Energetic and low-energy ion fluxes are characterized by stronger relative increase and decrease, respectively.

4. As a result, the total picture of the ion injection consist of a sequence of individual increases related evidently to the field-aligned current structures, activations of aurora, and the induction electric fields accelerating ions within a limited energy range.

5. Since the acceleration of the auroral electrons is also related to substrom activations, the large-scale picture of the injection of electrons and ions coincides in time. The time shift of individual acts is smoothed, and there appears a false impression on a unique mechanism of electron and ion injection.

6. The rapid growth of the plasma pressure prior to the explosive activation and the sharp decrease after it present an important factor of preparation of local substorm instabilities and the following expansion of a disturbance. The formed spatial pressure gradients, field-aligned currents, and current discontinuities are base elements of the substorm dynamics and can be directly related to these jumps in the plasma pressure and corresponding increases in ion fluxes.

## REFERENCES

1. Lazutin, L.L., Borovkov, L.P., Kozelova, T.V., *et al.*, Investigation of the Conjugacy between Auroral Breakup and Energetic Electron Injection, *J. Geophys. Res.*, 2000, vol. 105, pp. 18495–18504.

2. Lazutin, L.L., Kozelova, T.V., and Meredith, N. P., Studies of the Substorm on March 12, 1991: 2. Acceleration and Dynamics of Auroral Electrons, *Kosm. Issled.*, 2007, vol. 45, no. 2. (in press).

3. Tverskoi, B.A., Field-Aligned Currents in the Magnetosphere, *Geomagn. Aeron.*, 1982, vol. 22, no. 6, pp. 991–995.

4. Antonova, E.E., Field-Aligned Currents in the Polar Magnetosphere and Ionosphere, *Geomagn. Aeron.*, 1979, vol. 19, no. 4, pp. 676–679.

5. Hardy, D.A., Walton, D.M., Johnstone, A.D., *et al.*, Low Energy Plasma Analyzer, *IEEE Trans. Nucl. Sci.*, 1993, vol. 40, pp. 246–251.

6. Korth, A., Kremser, G., Wilken, B., *et al.*, Electron and Proton Wide-Angle Spectrometer (EPAS) on the CRRES Spacecraft, *J. Spacecr. Rockets*, 1992, vol. 29, pp. 609–614.

7. Singer, H.J., Sullivan, W.P., Anderson, P., *et al.*, Fluxgate Magnetometer Instrument on the *CRRES*, *J. Spacecr. Rockets*, 1992, vol. 29, no. 4, pp. 599–601.

8. Pudovkin, M.I., Zaitseva, S.A., Kornilova, T.A., and Pellinen, R.I., Dynamics of Aurora on the Equatorial Boundary of Auroral Zone, *Geomagn. Aeron.*, 1995, vol. 35, no. 1, pp. 47–54.

9. Kornilova, T.A., Kornilov, I.A., Pudovkin, M.I., and Kornilov, O.I., Two Types of Auroral Breakup, *Proc. 5th Intern. Conf. on Substorms, St. Petersburg, Russia, 16–20 May, 2000*, ESA SP-443, 2000, pp. 307–311.

10. Voronkov, I.O., Donovan, E.F., Dobias, P., *et al.*, Near-Earth Breakup in Substorms: Empirical and Model Constraints, *Sixth Intern. Conf. on Substorms*, Seattle, USA: Univ. of Washington, 2002, pp. 270–277.

11. Lui, A.T.Y., Extended Consideration of a Synthesis Model for Magnetospheric Substorms, in *Magnetospheric Substorms*, Kan, J.R., Ed., vol. 64 of *Geophysical Monographs*, 1991, pp. 43–60.

12. Lazutin, L., Korth, A., and Kozelova, T., Fast Bursts of High Energy protons and Their Role in Truggering of the Substorm Onset Instability, *Sixth Intern. Conf. on Substorms*, Seattle, USA: Univ. of Washington, 2002, pp. 340–346.

13. Lazutin, L., Kozelova, T., Rasinkangas, R., *et al.*, Radiation Belt Proton Contribution to Substorm Structure and Dynamics, in *Substorm-4*, Kokobun, S. and Kamide, Y., Eds., Tokyo: Terra, 1998, pp. 547–550.

14. Lazutin, L.L., and Kozelova., T.V., The Structure of Substorm Activations in the Quasi-Trapping Region, *Kosm. Issled.*, 2004, vol. 42, no. 4, pp. 323-344.

15. Rostoker, G., Akasofu, S.-I., Foster, J.C., *et al.*, Magnetospheric Substorms Definition and Signatures, *J. Geophys. Res.*, 1980, vol. 85, pp. 1663–1668.

16. Elphinstone, R.D., Observations in the Vicinity of Substorm Onset: Implications for the Substorm Process, *J. Geophys. Res.*, 1995, vol. 100, pp. 7037–7969.

17. Roux, A., Perreault, P., Robert, P., *et al.*, Plasma Sheet Instability Related to the Westward Traveling Surge, *J. Geophys. Res.*, 1991, vol. 96, pp. 17697–17707.

18. Samson, J.C., MacAulay, A.K., Rankin, R., *et al.*, Substorm Intensifications and Resistive Shear Flow-Ballooning Instabilities in the Near-Earth Magnetotail, *Third Intern. Conf. on Substorms, Versailles, France*, ESA SP-389, 1996, pp. 399–404.

19. Lui, A.T.Y., Current Disruption in the Earth's Magnetosphere: Observations and Models, *J. Geophys. Res.*, 1996, vol. 101, pp. 13067–13088.

20. Samson, J.C., Lyons, L.R., Newell, R.T., *et al.*, Proton Aurora and Substorm Intensifications, *Geophys. Res. Lett.*, 1992, vol. 19, no. 21, pp. 2167–2170.

21. Konradi, A., Semar, C.L., and Fritz, T.A., Substorm-Injected Protons and Electrons and the Injection Boundary Model, *J. Geophys. Res.*, 1975, vol. 80, pp. 543–552.

22. Isaev, S.I., *Morfologiya polyarnykh siyanii* (Morphology of Auroras), Leningrad: Nauka, 1968.

23. Fedorova, N.I., Tsirs, V., and Lazutin, L.L., Impulsive Brightness Increases of Proton Aurora before the Onset of Substorm Active Phase, *Geomagn. Aeron*, 1988, vol. 28, pp. 87–95.

24. Birn, J.M., Thomsen, M.F., Borovsky, J.E., *et al.*, Characteristic Plasma Properties during Dispersionless Substorm Injections at Geosynchronous Orbit, *J. Geophys. Res.*, 1997, vol. 102, pp. 2309–2324.

25. Rasinkangas, R., Sergeev, V.A., Kremser, G., *et al.*, Current Disruption Signatures at Substorm Onset Observed by CRRES, *Proc. of the Second Intern. Conf. on Substorms*, Kan, J.R., Craven, J., and Akasofu, S.-I., Eds., Fairbanks, Alaska: Geophys. Inst., 1994, pp. 595–599.

26. Kozelova, T.V. and Lazutin, L.L., Proton Injection at 6.6 RE in Early Evening Hours and Associated Phenomena, *Geomagn. Aeron.*, 1994, vol. 34, no. 6, pp. 37–44.

27. Kozelova, T.V., Lazutin, L.L., and Kozelov, B.V., Dipolization and Disturbance Currents in the Magnetosphere according to the *CRRES* Satellite Data, *Geomagn. Aeron.*, 1999, vol. 39, no. 1, pp. 15–26.

28. Antonova, E.E., Investigation of the Hot Plasma Pressure Gradients and the Configuration of Magnetospheric Currents from *INTERBALL*, *Adv. Space Res.*, 2003, vol. 31, no. 5, pp. 1157–1166.

29. Lyons, L.R., Voronkov, I.O., Ruohoniemi, J.M., and Donovan, E.F., Substorms: Externally Driven Transition to Unstable State a Few Minutes before Onset, *Sixth Intern. Conf. on Substorms*, Seattle, USA: Univ. of Washington, 2002, pp. 47–54.

30. Elphinstone, R.D., Murphree, J.S., and Cogger, L.L., What is a Global Auroral Substorm?, *Rev. Geophys.*, 1996, vol. 34, pp. 169–232.